



Article

# Effect of Bilastine on Diabetic Nephropathy in DBA2/J Mice

Roberta Verta <sup>1</sup>, Cristina Grange <sup>2</sup> , Maura Gurrieri <sup>1</sup>, Sara Borga <sup>1</sup>, Patrizia Nardini <sup>3</sup>,  
Monica Argenziano <sup>1</sup>, Corrado Ghè <sup>1</sup>, Roberta Cavalli <sup>1</sup>, Elisa Benetti <sup>1</sup>, Gianluca Miglio <sup>1</sup>,  
Benedetta Bussolati <sup>4</sup> , Alessandro Pini <sup>3,\*</sup>,† and Arianna Carolina Rosa <sup>1,\*</sup>,†

<sup>1</sup> Department of Scienza e Tecnologia del Farmaco, University of Turin, Via P. Giuria 9, 10125 Turin, Italy; robertaverta94@gmail.com (R.V.); maura.gurrieri@live.it (M.G.); sara.borga@edu.unito.it (S.B.); monica.argenziano@unito.it (M.A.); corrado.ghe@unito.it (C.G.); roberta.cavalli@unito.it (R.C.); elisa.benetti@unito.it (E.B.); gianluca.miglio@unito.it (G.M.)

<sup>2</sup> Department of Scienze Mediche, University of Turin, C.So Dogliotti 14, 10126 Turin, Italy; cristina.grange@unito.it

<sup>3</sup> Department of Clinical and Experimental Medicine, University of Florence, Viale Pieraccini 6, 50139 Florence, Italy; patrizia.nardini@unifi.it

<sup>4</sup> Department of Biotechnology and Health Sciences, Molecular Biotechnology Center University of Turin, Via Nizza 52, 10125 Turin, Italy; benedetta.bussolati@unito.it

\* Correspondence: alessandro.pini@unifi.it (A.P.); ariannacarolina.rosa@unito.it (A.C.R.); Tel: +39-0552758155 (A.P.); +39-0116707152 (A.C.R.)

† These authors contributed equally to this work.

Received: 26 April 2019; Accepted: 21 May 2019; Published: 24 May 2019



**Abstract:** Diabetic nephropathy is an unmet therapeutic need, and the search for new therapeutic strategies is warranted. Previous data point to histamine H<sub>1</sub> receptor as a possible target for glomerular dysfunction associated with long term hyperglycaemia. Therefore, this study investigated the effects of the H<sub>1</sub> receptor antagonist bilastine on renal morphology and function in a murine model of streptozotocin-induced diabetes. Diabetes was induced in DBA2/J male mice and, from diabetes onset (glycaemia  $\geq 200$  mg/dL), mice received bilastine (1–30 mg/kg/day) by oral gavage for 14 consecutive weeks. At the end of the experimental protocol, diabetic mice showed polyuria (+195.5%), increase in Albumin-to-Creatine Ratio (ACR, +284.7%), and a significant drop in creatinine clearance ( $p < 0.05$ ). Bilastine prevented ACR increase and restored creatinine clearance in a dose-dependent manner, suggesting a positive effect on glomerular filtration. The ultrastructural analysis showed a preserved junctional integrity. Preservation of the basal nephrin, P-cadherin, and synaptopodin expression could explain this effect. In conclusion, the H<sub>1</sub> receptor could contribute to the glomerular damage occurring in diabetic nephropathy. Bilastine preserved the glomerular junctional integrity, leading to the hypothesis of anti-H<sub>1</sub> antihistamines as a possible add-on therapy for diabetic nephropathy.

**Keywords:** histamine; histamine H<sub>1</sub> receptor; kidney; diabetes; slit diaphragm

## 1. Introduction

Diabetic nephropathy (DN) is a common and life-threatening microvascular complication of diabetes mellitus. It affects almost 30–45% of the overall diabetic patients [1,2]. DN is one of the major risk factors for end-stage renal disease (ESRD), cardiovascular diseases, and premature death without progression to ESRD [3–5]. Current therapies for DN are aimed to slow disease progression, mainly by ameliorating the glycemic control, inhibiting the renin–angiotensin aldosterone system, and changing the lifestyle [1,6]. However, despite the beneficial effects exerted by these approaches,

a large proportion of patients still undergo renal replacement therapy [1,7]. Therefore, further efforts should be done in order to effectively counteract DN.

In the last decades, our understanding of DN has been significantly enhanced. In particular, many events and mediators have been elucidated and clearly implicated in the process leading to the impairment of the glomerular filtration barrier [8]. Among them, abnormal histamine-mediated intercellular signaling has been indicated as a potential component of this process [9,10]. In particular, histamine overproduction was observed in diabetic patients [11]. Moreover, mice deficient in the histidine-decarboxylase (HDC) enzyme (responsible for histamine synthesis) showed a lower tendency to develop diabetes [12]. Finally, the same overproduction was found in several organs of diabetic rats, with the kidney being the second one in order of histamine increase [13]. Histamine renal content in diabetic condition has been correlated with an increase in HDC enzyme expression and activity [14,15]. Therefore, histamine in the kidney can derive from at least three sources: (i) circulating histamine, (ii) local production by epithelial cells, or (iii) infiltrating cells (including mast cells, although their level in the kidney is relatively low), with the intra-renal production being the major contributor [9,10]. Moreover, both *in vitro* and *in vivo* studies have provided compelling evidence on the expression and function of histamine receptors in the kidney. Functional histamine receptors in the kidney have a differential distribution along the nephron, with glomerulus expressing H<sub>1</sub> and H<sub>2</sub> receptors [16–18], proximal tubule H<sub>1</sub> and H<sub>4</sub> receptors [19], loop of Henlé H<sub>4</sub> receptor [20], and distal tubules H<sub>1</sub> and H<sub>2</sub> receptors [19]—while the H<sub>3</sub> receptor was found in the collecting ducts [21].

The cellular expression of H<sub>1</sub> receptor within glomerulus has been extensively evaluated. At this site, it was found on mesangial cells, where it mediates the histamine-promoted cell contraction [17]. This receptor type was also found on podocyte cell membrane, and its activation—analogue to what was observed for cultured retinal microvascular endothelial cells [22]—was related to the histamine-induced junctional-integrity disruption [18]. Collectively, this evidence indicates a role for the histamine-H<sub>1</sub> receptor axis in the onset of proteinuria and suggests the hypothesis that histamine affects the glomerular pore density, reducing the filtration surface area and leading to the decrease in the ultrafiltration coefficient [23]. This idea is sustained by the demonstration that H<sub>1</sub> receptor antagonism decreases proteinuria in a model of anti-glomerular basement membrane (GBM)-induced glomerulosclerosis [24]. In addition, consistent effects were described for (R)-cetirizine in a model of streptozotocin (STZ)-induced diabetes in rats [25]. Interestingly, comparable effects were exerted by both (R)-cetirizine and losartan on proteinuria (Urinary Protein Excretion, UPE; decrease) and creatinine clearance (CrCl; increase). However, given the relatively short extension of the follow-up adopted in this study (eight weeks) with regard to the rate of DN progression [25], these findings cannot be considered conclusive. Further data need to be collected to better understand the pathophysiological and pharmacological role of H<sub>1</sub> receptor in the context of DN. Therefore, this study aimed to assess the effects of bilastine on renal morphology and function in diabetic DBA2/J mice (the inbred strain of mice most susceptible to develop diabetic nephropathy following STZ administration [26]). Bilastine is a second-generation H<sub>1</sub> receptor antagonist, currently approved in many countries for the treatment of allergic disorders. Compared with (R)-cetirizine, bilastine is endowed with higher potency with no/minimal affinity for other receptor types [8]. Besides, the pharmacokinetic profile—an oral bioavailability of about 60–90%, the low extension of metabolic clearance, and the long duration of the effect (>24 h) [27,28]—make this drug a good candidate to be studied in a model of DN. Results collected in this study support the hypothesis that the H<sub>1</sub> receptor blockade reduces the glomerular damage preserving the junctional integrity at the Slit Diaphragm (SD).

## 2. Results

Two weeks after the last STZ injection (Figure 1), 90% of DBA2/J mice developed a diabetic status ( $\geq 200$  mg/dL) as measured by the 6 h fasting glycaemia. At the end of the study, a severe hyperglycaemia was reached in STZ group ( $450 \pm 56$  mg/dL vs.  $137 \pm 21$  mg/dL of the control group). The development of hyperglycaemia was accompanied by glycosuria (Table 1). Bilastine (1, 3, 10,

and 30 mg/kg/day by oral gavage from the onset of diabetes; Figure 1) did not significantly affect the hyperglycaemia in non-diabetic animals ( $147 \pm 24$  mg/dL) nor in diabetic ones ( $318 \pm 91$  mg/dL,  $364 \pm 74$  mg/dL,  $293 \pm 52$  mg/dL, and  $319 \pm 87$  mg/dL, respectively) or glycosuria (Table 1).

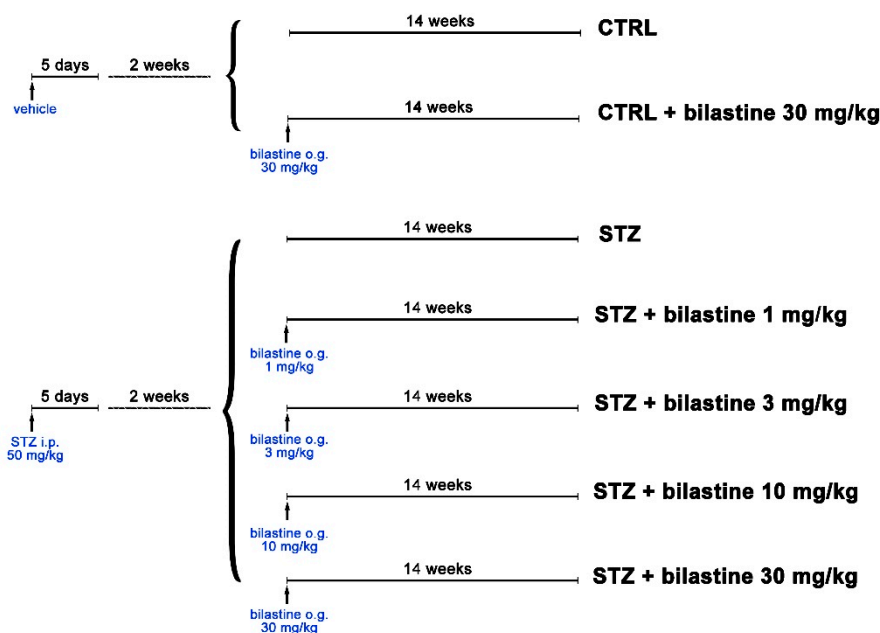


**Figure 1.** Diagram of the experimental design describing group allocation ( $n = 10$  animals/per group). CTRL = control; STZ = streptozotocin; i.p. = intraperitoneal injection; o.g. = oral gavage.

**Table 1.** Renal function parameters at week 14 after diabetes onset.

|                                    | CTRL            | CTRL + Bilastine<br>30 mg/kg | STZ                | STZ + Bilastine (mg/kg) |                  |                        |                      |
|------------------------------------|-----------------|------------------------------|--------------------|-------------------------|------------------|------------------------|----------------------|
|                                    |                 |                              |                    | 1                       | 3                | 10                     | 30                   |
| Glucosuria <sup>o</sup><br>(mg/dL) | n.d.            | n.d.                         | $1500 \pm 224$     | $1000 \pm 0$            | $1188 \pm 188$   | $1143 \pm 143$         | $1500 \pm 289$       |
| Urine<br>volume (mL)               | $6.8 \pm 0.7$   | $6.4 \pm 0.7$                | $19.8 \pm 1.1^*$   | $22.5 \pm 2.9^*$        | $17.5 \pm 3.6^*$ | $21.6 \pm 2.3^*$       | $32.5 \pm 2.5^*$     |
| Leukocyte                          | -               | -                            | -                  | -                       | -                | -                      | -                    |
| Urine pH <sup>o</sup>              | $6.5 \pm 0.0$   | $6.4 \pm 0.1$                | $6.0 \pm 0.2$      | $6.0 \pm 0.2$           | $6.2 \pm 0.1$    | $6.0 \pm 0.1$          | $5.9 \pm 0.1$        |
| UPE<br>(mg/mL)                     | $0.8 \pm 0.1$   | $0.8 \pm 0.1$                | $3.2 \pm 0.2^*$    | $3.7 \pm 0.5^*$         | $2.0 \pm 0.4$    | $2.8 \pm 0.4^*$        | $3.6 \pm 1.1^*$      |
| ACR<br>( $\mu$ g/mg)               | $66.9 \pm 6.0$  | $60.4 \pm 9.7$               | $257.4 \pm 27.2^*$ | $150.6 \pm 33.8$        | $101.4 \pm 23.1$ | $132.2 \pm 9.8$        | $90.3 \pm 40.9^{\#}$ |
| CrCl<br>(mL/min)                   | $0.13 \pm 0.01$ | $0.14 \pm 0.01$              | $0.05 \pm 0.01^*$  | $0.05 \pm 0.01^{\S*}$   | $0.09 \pm 0.03$  | $0.14 \pm 0.01^{\S\#}$ | $0.15 \pm 0.02^{\#}$ |

<sup>o</sup> = semi-quantitative analysis by dip-stick; UPE = Urinary Protein Excretion; ACR = Albumin-to-Creatinine Ratio; CrCl = Creatinine Clearance; \* vs. CTRL  $p < 0.05$ ; # vs. STZ;  $p < 0.05$ ;  $\S$  vs. STZ + 30 mg/kg;  $p < 0.05$ ; n.d. = under detection limit; - = negative.

Only control animals gained weight, while all diabetic animals displayed significant weight loss over time (Figure 2), even when accounting for differences in food consumption (data not shown). Bilastine did not affect body weight in non-diabetic animals (data not shown) nor in diabetic ones (Figure 2).

### 2.1. Bilastine Effects on Renal Function

For the renal function evaluation, bilastine did not affect any of the measured parameters when administered to non-diabetic animals (Table 1). In comparison with control animals, a significant increase in the 24 h urine volume was measured in STZ-treated animal on week 14 (+196.8%;  $p < 0.05$ ). This change was not prevented by bilastine (Table 1). No sign of infection or obstruction was found,

as demonstrated by the negativity for leukocyte presence. In diabetic mice, irrespective of the drug treatment, a trend towards a decrease in the urine pH compared to the control was observed (Table 1). UPE and Albumin-to-Creatinine Ratio (ACR) were significantly increased in diabetic animals compared to the control ( $p < 0.05$ ). The drug was unable to prevent UPE but prevented the development of ACR with a significant effect at the highest dose tested (30 mg/kg). Moreover, a significant drop in CrCl of diabetic mice was measured (Table 1). Bilastine treatment prevented the CrCl reduction in a dose-dependent manner, with the 10 and 30 mg/kg doses restoring CrCl levels to the control (Table 1). Collectively, these data suggest that bilastine could exert a protective effect on renal function.

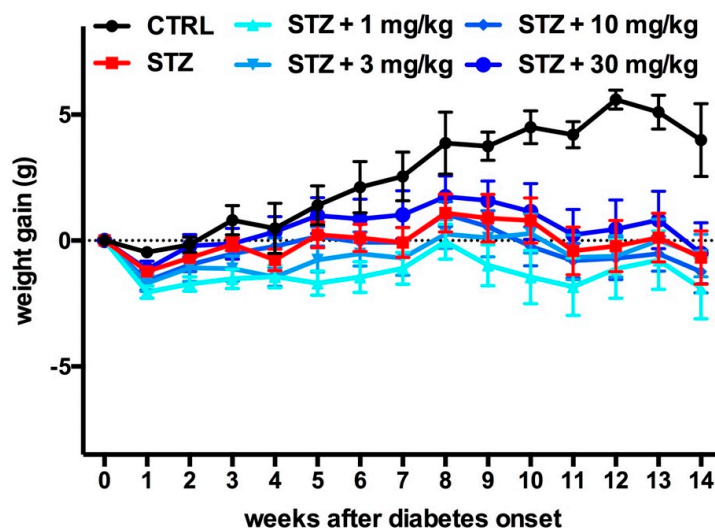


**Figure 2.** Effect of bilastine on weight gain. Body weight was monitored on a weekly basis, starting from diabetes development (week 0, glycemia  $\geq 200$  mg/Dl for 90% of diabetic animals) throughout the experimental period and weight gain was estimated. Data are expressed as mean  $\pm$  S.E.M. ( $n = 10$ /group).

## 2.2. Bilastine Effect on Glomerular Structure Alterations

To assess the effect of bilastine on glomerular structure integrity, the morphological examination of Periodic Acid–Schiff (PAS) staining was performed. The light microscope analysis revealed lobulated glomeruli with moderate mesangial matrix expansion (Figure 3) in the STZ group, thus indicating moderate diabetes-induced damage. No lesions consisting of Kimmelstiel–Wilson nodules were present in the kidneys of diabetic mice. Bilastine administration significantly reduced the mesangial matrix expansion, irrespectively to the dose (Figure 3), thus suggesting that bilastine could prevent glomerular damage.

The ultrastructural evaluation of renal samples is reported in Figure 4. The control group revealed normal glomerular capillary tuft arrangement (Figure 4, Panel A), intact filtration barrier with regular sized, well-aligned podocyte foot processes (FP), and uniform filtration pores (Figure 4, Panel a). In the STZ-induced diabetic mice, the capillary tufts showed irregular fold (Figure 4, Panel B), with areas of the capillary loop surface covered by damaged podocytes. In particular, the FP were diffusely effaced, with irregular size, shape, and variation in the width of the pores (Figure 4, Panels B and b), indicating podocyte loss. No signs of GBM thickening were appreciated in the kidney of diabetic mice. In bilastine treated mice, the architecture of glomerular capillary tuft was preserved (Figure 4; Panels C, D, E, and F). In particular, the drug at 3, 10, and 30 mg/kg was able to structurally preserve the filtration barrier, preventing the effacement of podocyte FP, which appeared to be regular sized and shaped and not detached from the GBM (Figure 4; Panels c, d, e, and f). Also, the observation of filtration pores along the GBM confirmed the protective effect exerted by bilastine. These data show that  $H_1$  receptor antagonism could preserve the integrity of the filtration barrier.

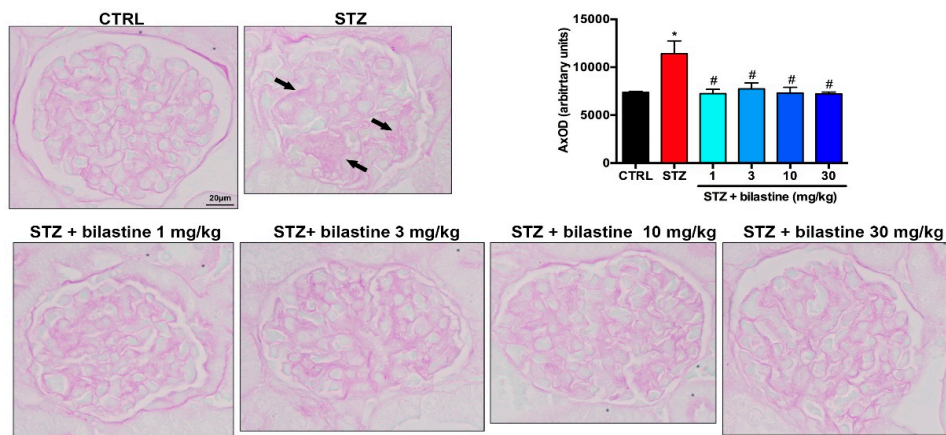


**Figure 3.** Effect of bilastine on glomerular morphology. Representative micrographs at 100× magnification of PAS stained renal sections. Arrows highlight mesangial matrix expansion. The image is representative of 20 microscopic fields/specimen and 10 animals/group. The densitometric analysis is expressed as the mean ± S.E.M. ( $n = 10$ ); \*  $p < 0.05$  vs. CTRL; #  $p < 0.05$  vs. STZ.

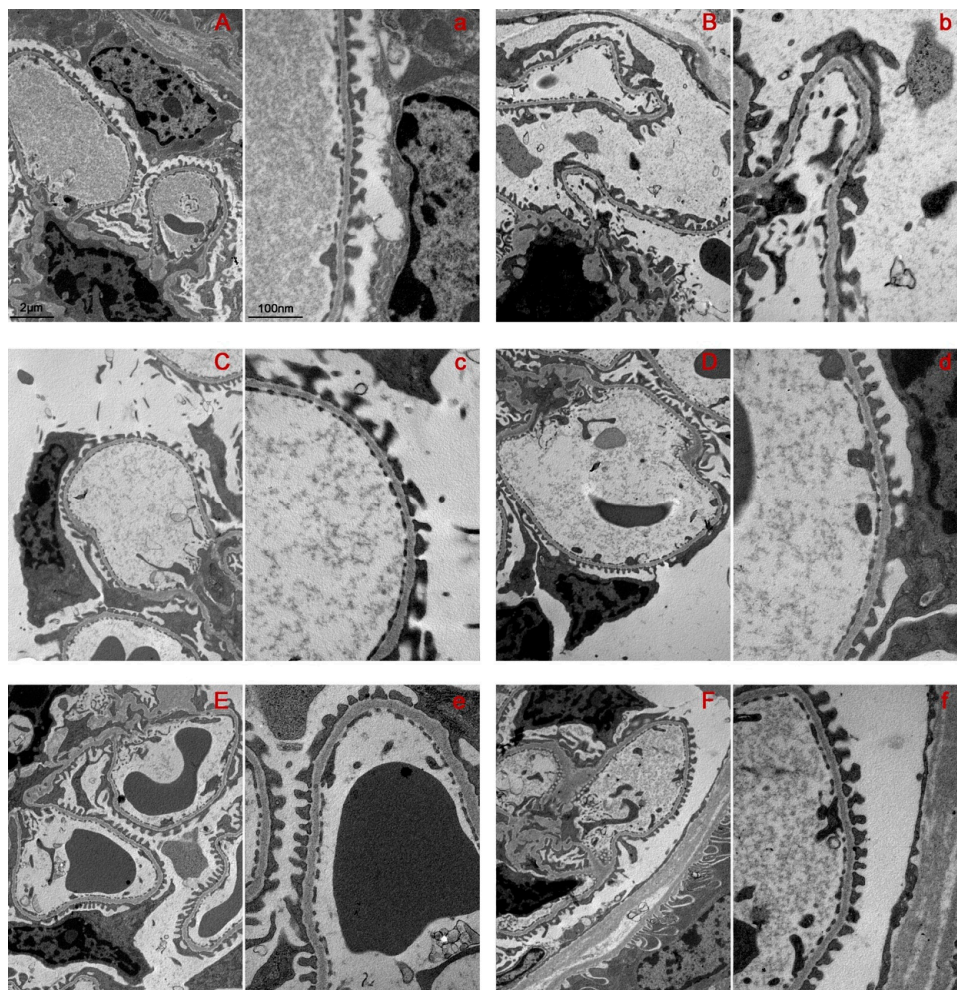


**Figure 4.** Effect of bilastine on glomerular morphology. Representative electron microscope micrographs showing ultrathin podocyte sections. Micrographs at 10 K (Capital letters) and 25 K (Lower case letter) magnification are representative of 5 animals/group. **A** and **a** = CTRL; **B** and **b** = STZ; **C** and **c** = STZ + bilastine 1 mg/kg; **D** and **d** = STZ + bilastine 3 mg/kg; **E** and **e** = STZ + bilastine 1 mg/kg; **F** and **f** = STZ + bilastine 1 mg/kg.

### 2.3. Bilastine Effect on Slit Diaphragm and Cytoarchitecture Protein Expression

The effect of bilastine on junctional proteins involved in the maintenance of the SD integrity, nephrin (Figure 5, Panels A and B), P-cadherin (Figure 5, Panels A and C), podocin (Figure 5, Panels A and D) and synaptopodin (Figure 5, Panels A and E), were evaluated by immunoblotting. As expected, diabetic animals showed a down-regulation of all these proteins (Figure 5). Bilastine partially prevented these dysregulations. Indeed, the highest dose was effective in preserving the basal levels of nephrin, P-cadherin and synaptopodin (Figure 5). On the contrary bilastine was not able to prevent podocin loss (Figure 5, Panel D), albeit a trend towards a protective effect was observed. Therefore, the data suggests that bilastine preserves, at least in part, the junctional integrity of the SD.

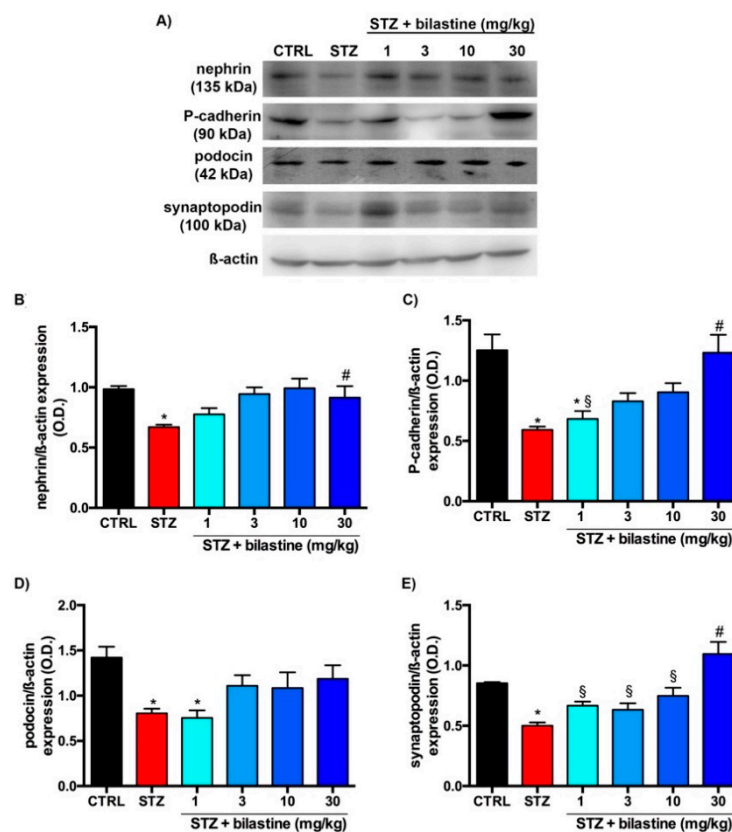


**Figure 5.** Effect of bilastine on podocyte protein expression. Representative radiograph of nephrin, P-cadherin, podocin, and synaptopodin expression in kidney tissue determined by immunoblotting (A). The densitometric analysis of nephrin (B), P-cadherin (C), podocin (D), and synaptopodin (E) was performed and expression levels, normalized to  $\beta$ -actin, are expressed as the mean  $\pm$  S.E.M. of 5 animals/group; \*  $p < 0.05$  vs. CTRL, #  $p < 0.05$  vs. STZ; §  $p < 0.05$  vs. STZ + bilastine 30 mg/kg.

### 2.4. Bilastine Effect on NHE3 Expression

In order to better elucidate the effects of bilastine on tubular reabsorption, we investigated the expression of the sodium–hydrogen exchanger (NHE)3 protein expressed on the brush border membrane of renal proximal tubules and responsible for active transcellular reabsorption of  $\text{NaHCO}_3$  and  $\text{NaCl}$  [29]. The immunofluorescence analysis revealed an increase in the apical expression of NHE3 in diabetic animals compared to the control group. Bilastine-treated mice showed a lower immunopositivity suggestive of a prevention of NHE3 over-expression, but control levels were not restored (Figure 5, Panel A). These data were confirmed by immunoblotting analysis. Diabetic mice displayed a significant up-regulation of NHE3 expression (Figure 6, Panels B and C). Bilastine had no significant effect on NHE3 expression, albeit a trend towards a protective effect was observed.

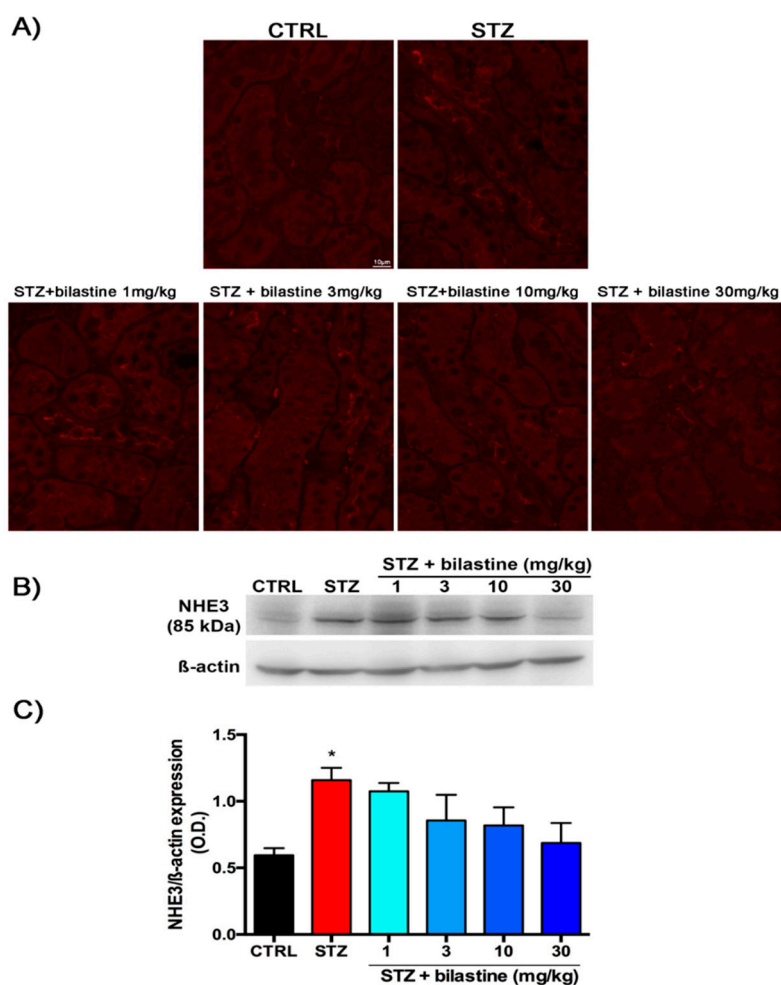


**Figure 6.** Effect of bilastine on NHE3 tubular expression. Micrographs representative of NHE3 expression on tubular epithelial cells determined by immunofluorescence (63× magnification from 10 animals/group) (A). Representative radiograph of NHE3 expression in kidney tissue determined by immunoblotting (B). Densitometric analysis of NHE3 expression determined by immunoblotting analysis. Expression levels, normalized to β-actin, are expressed as the mean ± S.E.M. of 5 animals/group; \*  $p < 0.05$  vs. CTRL, #  $p < 0.05$  vs. STZ (C).

### 2.5. Bilastine Effect on Tubular Infiltration and Renal Fibrosis

According to the already known pro-inflammatory and profibrotic properties of histamine, and of H<sub>1</sub> receptor activation, the effect of bilastine on the presence of infiltrating immune cells was evaluated. As shown in Figures 7 and 8, the morphological evaluation of May–Grünwald–Giemsa and hematoxylin and eosin staining showed a moderate hyper-cellularity consistent with pro-inflammatory infiltration (leukocyte and neutrophils in particular) in the STZ group. This effect was paralleled by a significant but moderate interstitial fibrosis, as demonstrated by picosirius red staining (Figure 9). The administration of bilastine reduced the hyper-cellularity (Figure 7) and significantly blunted the collagen deposition induced by STZ-induced hyperglycaemia (Figure 9), irrespective of the dose.

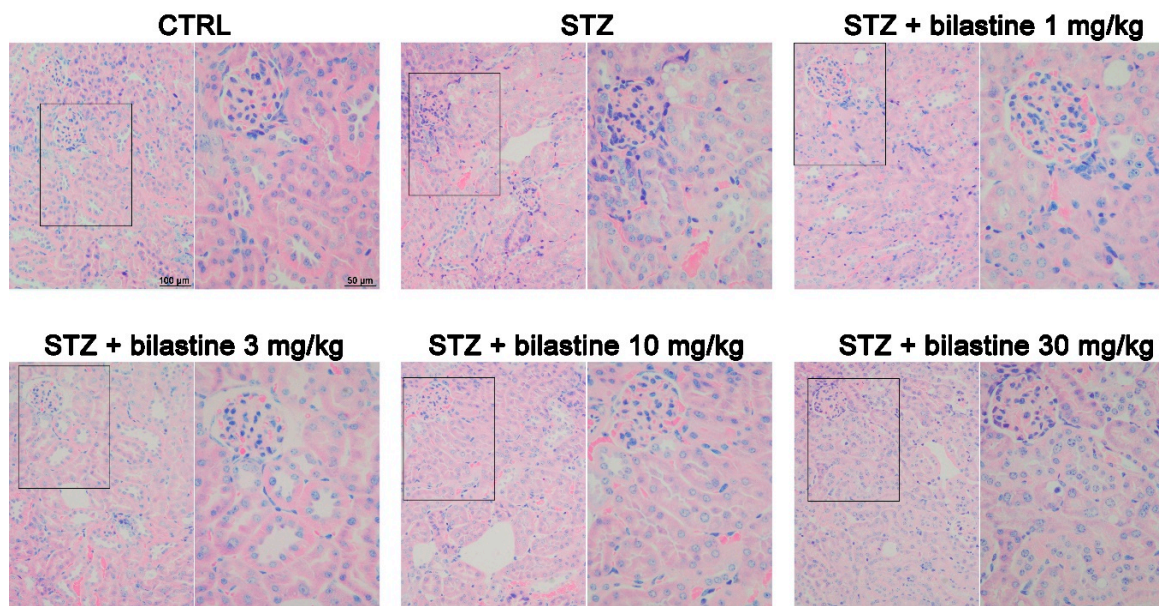


**Figure 7.** Effect of bilastine on tubular interstitial infiltration. May–Grünwald–Giemsa staining from renal sections. Micrographs at 20× or 40× (insert) magnification are representative of 10 animals/group.

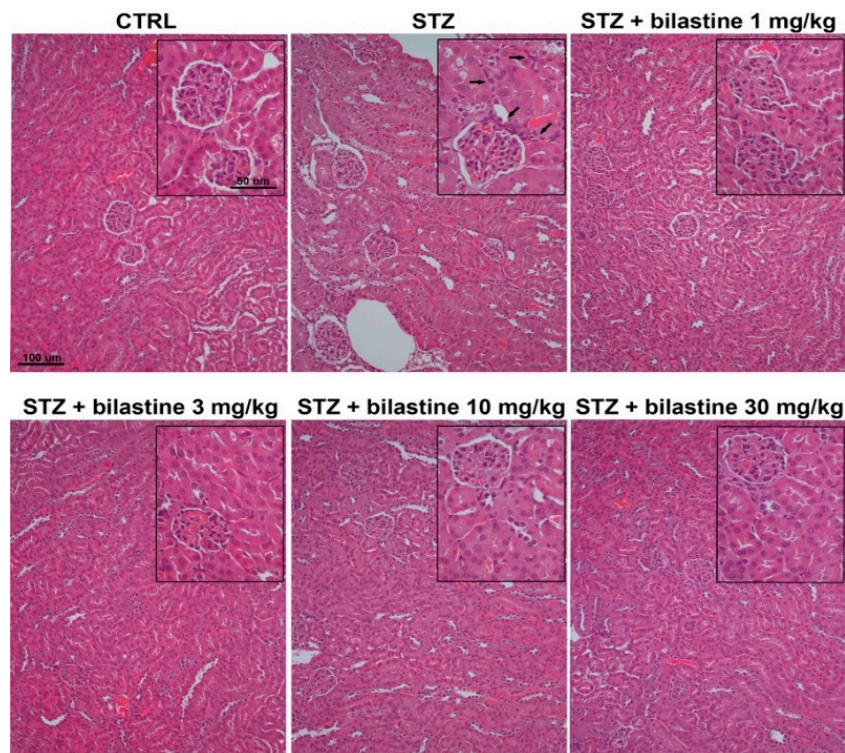


**Figure 8.** Effect of bilastine on tubular interstitial infiltration. Hematoxylin and eosin staining from renal sections. Arrows highlight infiltrating cells. Micrographs at 20× or 40× (insert) magnification are representative of 10 animals/group.



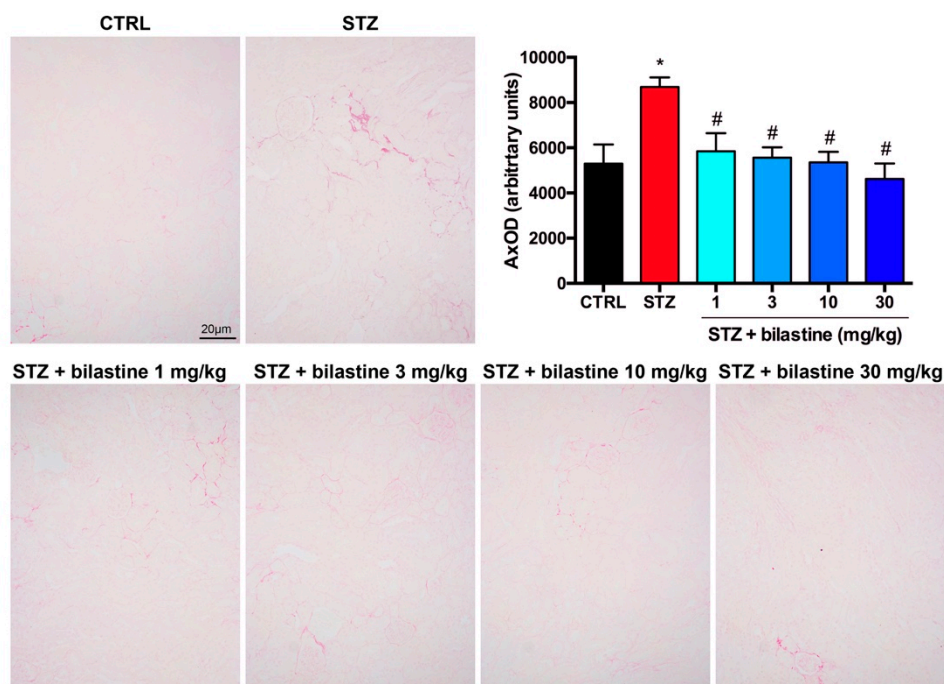


**Figure 9.** Effect of bilastine on tubular fibrosis. Collagen deposition in the renal interstitium evaluated by picosirius red staining. Micrographs at 20× magnification are representative of 10 animals/group (20 microscopic fields/specimen). The densitometric analysis is expressed as the mean ± S.E.M. ( $n = 10$ ); \*  $p < 0.05$  vs. CTRL, #  $p < 0.05$  vs. STZ.

### 3. Discussion

Data reported herein demonstrated that bilastine—preserving the junctional integrity at the glomerular SD—prevents the increase of ACR and the reduction of CrCl in diabetic animals. Interestingly, these data are consistent with previous data by Ichikawa and Brenner (1979) [23] indicating a decrease in the ultrafiltration coefficient following  $H_1$  receptor activation. In our experimental setting, just a mild renal injury, not recapitulating all the features of DN, was obtained after 14 weeks from the onset of diabetes ( $\geq 200$  mg/dL in 90% of STZ-treated animals), and a preventive therapeutic approach was used (bilastine was administered as soon as the onset of diabetes). In this model, we obtained a modest matrix mesangial expansion and no thickening of the GBM, however, a consistent podocyte FP effacement and podocyte loss was revealed. The drug prevented these detrimental events.

Interestingly, an apparent discrepancy between functional and morphological data appears. Indeed, while only bilastine 30 mg/kg showed a full protection of renal function, matrix mesangial expansion and collagen deposition were significantly affected by bilastine, irrespective of the dose. However, these are both pro-fibrotic events that could be related to the general anti-inflammatory effect of bilastine, also confirmed in this study in terms of reduction of infiltrating cells. On the contrary, the biochemical evaluation (nephrin, synaptopodin, and P-cadherin expression), keeping with the functional analysis, reached statistical significance only by bilastine at 30 mg/kg. Therefore, we could speculate that histamine is a trigger stimulus for the renal inflammatory response induced by hyperglycaemia, but is also a contributor to the podocyte junctional integrity, to which other mediators, such as angiotensin II [29], participate as well. Consistently, no different effects were shown between (R)-cetirizine and losartan on renal protection in diabetic rats [25].

The observed effect of bilastine is possibly due to the haemodynamic regulation induced by blocking  $H_1$  receptor. Indeed, histamine can affect glomerular haemodynamics [9,10] mostly through  $H_1$  receptor [30], and podocytes respond to intracapillary pressure with the loss of the interdigitating foot process pattern [31]. In our model, bilastine was demonstrated to prevent the podocyte FP effacement. This event was sustained by a conserved expression of different proteins involved

in the SD maintenance—in particular, the two junctional proteins nephrin and P-cadherin and the actin binding protein synaptopodin. However, all these changes can also be the consequence of a direct effects of bilastine on podocyte, a cell type expressing H<sub>1</sub> receptor [18]. Indeed, in a previous *in vitro* study, H<sub>1</sub> receptor was already demonstrated to modulate P-cadherin expression in human podocytes [18]. In this study, H<sub>1</sub> receptor activation was demonstrated to generally affect the intra-podocyte junctional machinery and also to down-regulate Zonula Occludens (ZO)-1 expression [18]. Therefore, direct effect(s) on SD protein expression could also occur *in vivo*. Moreover, a contribution of the H<sub>1</sub> receptor expressed at the mesangial site [17] cannot be ruled out.

Therefore, even considering the previous data from others, we suggest that H<sub>1</sub> receptor antagonism could exert a renal protective effect by: (i) The maintenance of glomerular intracapillary pressure [30], (ii) the preservation of constitutive levels of the podocyte junctional-related proteins, and (iii) the prevention of mesangial contraction [17]. These effects are far behind any glycemic control as bilastine, different to (R)-cetirizine [25], was shown to not affect the glycemic status.

The relationship between histamine signaling and glomerular junctional integrity is an intriguing albeit poorly investigated point. At the molecular level, a plausible link could be found in the role played by Protein Kinases C (PKC) in mediating both the histamine cellular effects and the maintenance of the SD integrity. Indeed, as already reported, H<sub>1</sub> receptor stimulation induces an increase in inositol 1,4,5-trisphosphate (IP3) second messenger in podocytes [18]. IP3 is known to activate PKC, which plays a crucial role in the preservation of the SD integrity [32]. In particular, PKC is involved in the regulation of SD junctional protein expression, such as P-cadherin [33]. Therefore, we can speculate that an abnormal stimulation of the H<sub>1</sub> receptors expressed by podocytes could alter the PKC activity, which in turn could contribute to the disruption of the SD integrity. By antagonizing the effects exerted by histamine, bilastine could prevent all these events. Interestingly, no functional effects on renal function were observed when bilastine was administered to non-diabetic mice. Therefore, a possible involvement of inverse agonism of bilastine in the therapeutic effects is unlikely.

The involvement of the histamine H<sub>1</sub> receptor reported here recalls to the possible analogy between metabolic diseases and allergies [34]. Indeed, the association between the prevalence of Type 1 diabetes and allergic diseases or sensitization [35] has been reported. In homology with asthma, the mechanism(s) underlying this association can be related not only to Th2 driven, but also to Th2 non-driven events [34,35]. In both cases, the immuno-metabolic dysfunction is the underlying event. Nevertheless, the release of histamine from mast-cells during an allergic response has been associated to the development of metabolic cardiovascular dysfunctions such as atherosclerosis [36]. Therefore, it could be suggested that the increased histamine levels related to diabetic condition trigger an immuno-metabolic dysfunction, which in turn could contribute to microvascular complications, including the DN.

Considering the data previously obtained on the H<sub>4</sub> receptor blockade in a similar diabetic model [15], the effects observed at the glomerular level after bilastine treatment are open to many interesting interpretations of the role of histamine in renal pathophysiology, allowing researchers to hypothesize different roles of H<sub>1</sub> and H<sub>4</sub> receptors. Indeed, the H<sub>4</sub> receptor blockade by JNJ39758979 was demonstrated to preserve proximal tubular reabsorption, preventing megalin loss and NHE3 increase in the tubules of diabetic mice. Moreover, water volume was significantly and dose-dependently reduced [15]. These data were consistent with the prevalent H<sub>4</sub> receptor expression on the tubule [20], especially at the proximal tract [19]. Also, H<sub>1</sub> receptor is expressed in the tubule [19]. However, bilastine did not prevent the decrease in urine pH and the increase in urine volume or in proteinuria, despite the beneficial effects on ACR and CrCl. Therefore, H<sub>1</sub> receptor activation could not contribute to the detrimental effects on the tubular reabsorptive machinery, and this hypothesis was confirmed by the effect on NHE3 expression. NHE3 is a proximal tubular transporter, which facilitates sodium reabsorption and proton secretion, thus participating in the acid–base balance [29]. It is known to be up-regulated by a hyperglycaemic status, and its expression is inversely correlated to that of the protein responsible for albumin re-uptake, megalin [37]. In our study, diabetic mice showed a significant

NHE3 over-expression compared to the control animals, while bilastine was not effective in preventing NHE3 increase, although a slight but not significant beneficial effect was observed for bilastine at 30 mg/kg. This unexpected result could explain the lack of efficacy on protein excretion and urinary pH value. The high protein outflow and the low pH, even in the presence of bilastine, could account for the observed polyuria.

However, the study has some limitations including: (i) The one end-point design, which does not allow us to evaluate at which stage of DN onset bilastine exerts its effects; and (ii) the administration of bilastine at the early onset of diabetes, and not after DN development. This design configures a preventive approach more than a therapeutic one, and no conclusion on the efficacy of bilastine after the onset of the renal complication can be extrapolated. Therefore, for a final conclusion on the possible therapeutic use of bilastine as an active agent against DN, further studies based on a therapeutic approach (bilastine administration after DN development) are needed.

#### 4. Materials and Methods

##### 4.1. Materials

All chemicals, not otherwise indicated and rabbit polyclonal anti- $\beta$ -actin antibody (A2066), were from Sigma Aldrich (St. Louis, MO, USA). The Glucocard MX Blood Glucose Meter was from A. Menarini Diagnostic (Florence, Italy). The Albumin enzymatic immunoassay kits ELISA Quantification Set (E90-134) was from Bethyl Laboratories Inc. (Montgomery, TX, USA). The Urine Strips were from GIMA S.p.a. (Gessate, MI, Italy). The goat polyclonal anti-nephrin antibody (N-20; sc-19000), the goat polyclonal anti-synaptopodin (N-14; sc-21536), rabbit polyclonal anti-P-cadherin (H-105; sc-7893), and rabbit polyclonal anti-podocin (H-120; sc-21009) as well as UltraCruz Autoradiography Film were from Santa Cruz Biotechnology (Dallas, TX, USA); the rabbit polyclonal anti-NHE3 (GTX41967, lot number 821700650) was from Gentex (Santa Antonio, TX, USA). The donkey polyclonal anti-rabbit Fluor 594 AffiniPure (711-585-152) was from Jackson ImmunoResearch Laboratories (Baltimore Pike, West Grove, PA, USA). The rabbit peroxidase-labelled secondary antibody was from Cell Signaling Technology Inc. (Danvers, MA, USA). The BCA™ Protein Assay Kit was from ThermoFisher Scientific (Waltham, MA, USA). The Immobilon® PVDF transfer membrane was from Merck Millipore (Milan, Italy). The Acrylamide/Bis solution 29:1 and the Albumin bovine modified Cohn Fraction V (BSA), pH 7.0 were from SERVA (Heidelberg, Germany). The WesternBright™ Quantum detection kit for the chemiluminescent detection and the Western Blot Strip-it Buffer were from Advansta (Menlo Park, CA, USA).

Bilastine was obtained by dissolution of the commercial drug Robilas® (A. Menarini, Industries Farmaceutiche Riunite s.r.l., Florence, Italy) with *N*-methyl-pyrrolidone (final concentration 0.1%), a solubilizer with low toxicity both orally and parenterally (Solubility Improvement of Drugs using *N*-Methyl Pyrrolidone).

##### 4.2. Animal Care and Ethics Statement

Five six-week-old male DBA2/J mice (Charles River Laboratories, Calco, Italy) were maintained in compliance with the European Council directives (No. 2010/63/EU) and with the Principles of Laboratory Animal Care (NIH No. 85-23, revised 2011). The animals were kept at constant environmental and nutritional conditions at  $25 \pm 2$  °C with alternating 12 h light and dark cycles and fed with a standard diet during a 1-week adaptation period. They were fed with a standard pellet diet (Piccioni, Settimo Milanese, Milan, Italy) and watered ad libitum. The scientific project was approved by the Ethical Committee of Turin University and by the Italian Ministry of Health (Authorization No. 279/2016 PR, approval date: 17/03/2016). The minimum sample size of 10 animals/group was determined by applying the Fleiss test for an unmatched case-control study as power analysis. The confidence interval was 90%, the power was at 85%, and the alpha level was set at 0.05. This design provides the power to investigate the differences in renal function between the different groups.

#### 4.3. Experiment Protocol

Diabetes was induced in DBA2/J 18.8–20.7 g mice by a multiple low-dose STZ-intraperitoneal injection (50 mg/kg per day STZ freshly made in 0.1 mol/L citrate buffer, pH 4.5) for 5 consecutive days. Control animals were treated with vehicle alone (Figure 1). Diabetes was defined as fasting blood glucose level  $\geq 200$  mg/dL, and the onset of diabetes was evaluated by measuring 6 h fasting blood glucose using a Glucocard MX Blood Glucose Meter. After onset of diabetes, the selective H<sub>1</sub> receptor antagonist bilastine was administered daily for 15 weeks as a water solution by oral gavage at 1, 3, 10, 30 mg/kg (Figure 1). Weight, food, and water intake were reordered on a weekly basis. At the end of the experimental period, mice were anaesthetized with isoflurane and killed by cardiac exsanguination. Blood and kidneys were collected for biochemical and morphological analyses on renal function. Data recording and data analysis were blinded to both the operators and the analysts, with only the individual administered the drug aware of the drug treatments given. Animal specimens were randomly labelled by a unique numeric code by A.C.R., to guarantee blind tissue sample processes.

#### 4.4. Renal Function Evaluations

Twenty-four hour urine collection was performed using metabolic cages. Urine volume and pH were determined. UPE was measured by Bradford method using Bovine Serum Albumin as the standard. Albuminuria was determined by ELISA. Creatinine was measured on both plasma and urine samples by a High-Performance Liquid Chromatography (HPLC) reverse-phase method as previously described [15].

#### 4.5. Morphological Analysis

Kidneys specimens were fixed by immersion in 4% paraformaldehyde, 0.1 M phosphate buffered saline (PBS) pH 7.4 overnight, embedded in paraffin. Therefore, the specimens were cut in 5  $\mu$ m thick sections. Hematoxylin and eosin staining were carried out in order to analyze the gross tissue organization, May–Grunwald–Giemsa staining to evaluate leukocyte infiltration, while PAS reaction (0.5% Periodic Acid Solution) was performed to quantify mesangial matrix expansion. Moreover, renal fibrosis was assessed by picrosirius red staining, a reliable and sensitive method for the quantitative evaluation of collagen fibers [38], carried out using 0.1% picrosirius red. The morphometrical measurements of PAS and picrosirius red stained sections were examined and pictures were acquired with Zeiss Axioskop microscope (Zeiss, Mannheim, Germany). In particular, 20 microscopical fields/specimen were randomly selected and were digitalized at 100 $\times$  and 20 $\times$  magnifications for PAS and picrosirius red, respectively. Data analysis and measurements were performed with ImageJ software (version 1.48v; National Institutes of Health, Bethesda, MD, USA).

#### 4.6. Transmission Electron Microscopy

Renal biopsies were cut in 1 mm<sup>3</sup>, fixed at 4 °C in 4% glutaraldehyde (phosphate buffered, pH 7.2), post-fixed in 1% osmium tetroxide and embedded in Epon 812 using gelatin capsules. Semi-thin sections were obtained with an LKB NOVA ultra-microtome (Stockholm, Sweden), stained with a solution of toluidine blue in 0.1 mol/L borate buffer, and observed under a light microscope to check the area of interest selecting at least three renal glomeruli per biopsy. Ultrathin sections were stained with Uranylless (Electron microscopy sciences, Hatfield, PA, USA) and alkaline bismuth sub-nitrate and then examined under a JEM 1010 electron microscope (Jeol, Tokyo, Japan) at 80 kV.

#### 4.7. Immunofluorescence Analysis

NHE3 immunoreactivity was determined on 5  $\mu$ m thick tissue sections. The sections were deparaffinized and re-hydrated, followed by microwave antigen retrieval in 10 mM sodium citrate, pH 6.0. In order to quench the autofluorescence and to minimize the non-specific binding, sections were incubated in 2 mg/mL glycine for 10 min and then for 20 min at room temperature with 1.5%

bovine serum albumin in PBS pH 7.4. Sections were subsequently incubated overnight with rabbit polyclonal anti-NHE3. The immunoreactions were revealed by incubation with donkey anti-rabbit Fluor 594-conjugated IgG for 2 h at room temperature. Negative controls were carried out by omitting the primary antiserum. The immunoreaction products were observed, and pictures were acquired with Apotome systems (Zeiss) using 63× magnification.

#### 4.8. Immunoblotting

Kidney randomly selected from 5 animals/group were lysed in cold buffer (10 mM Tris/HCl pH 7.4, 10 mM NaCl, 1.5 mM MgCl<sub>2</sub>, 2 mM Na<sub>2</sub> EDTA, 1% Triton X-100), supplemented with 10× Sigmafast Protease Inhibitor cocktail tablets. Total protein content was measured spectrophotometrically using a micro-BCA™ Protein Assay Kit. Forty micrograms of total proteins were randomly electrophoresed by SDS-PAGE and blotted onto PVDF membranes. The membranes were incubated overnight at 4 °C with rabbit polyclonal anti-podocin, P-cadherin, and NHE3 or with goat polyclonal anti-nephrin and anti-synaptopodin. The rabbit polyclonal anti β-actin antibodies were used as a control. The bands were detected using rabbit or goat peroxidase-labelled secondary antibody and enhanced by WesternBright™ Quantum detection kit. Chemiluminescence signal was captured by the CDD camera ChemiDoc™ (Bio-Rad, Segrate, Italy) or, alternatively, by X-ray film exposure. The densitometric analysis was performed by ImageJ software.

#### 4.9. Statistical Analysis

Data were reported as mean values (± standard error of the means, S.E.M.). Statistical analysis was performed using one-way analysis of variance (ANOVA). PostHoc Calculations applying the Tukey's multiple comparisons test were made with Prism 6 statistical software (GraphPad Software, Inc., San Diego, CA, USA). Significance was set at probability value (*p*) of < 0.05.

### 5. Conclusions

In conclusion, our data strongly support the hypothesis that H<sub>1</sub> receptor could contribute to the glomerular damage occurring in DN. Bilastine was able to preserve, at least partially, the junctional integrity of the SD, through both direct and indirect effects on podocyte cytoarchitecture. Therefore, there is some scope to hypothesize the use of anti-H<sub>1</sub> receptor antagonists as add-on therapy for DN, however a comparative analysis of different anti-H<sub>1</sub> antihistamines in DN is still needed.

**Author Contributions:** Conceptualization, A.C.R., A.P., and R.V.; Methodology, A.C.R., A.P., C.G. (Cristina Grange), C.G. (Corrado Ghè), and R.C.; Formal Analysis, E.B.; Investigation, R.V., M.G., S.B., M.A., and P.N.; Writing—Original Draft Preparation, R.V. and A.P.; Writing—Review and Editing, G.M., A.C.R., and B.B.; Visualization, P.N. and C.G. (Cristina Grange); Supervision, A.C.R. and A.P.; Funding Acquisition, A.C.R. and A.P.

**Funding:** This work was funded by the University of Turin (ex60% 2015 and ex60% 2016) and the University of Florence (ex60% 2017).

**Conflicts of Interest:** The authors declare no conflict of interest.

#### Abbreviations

|      |                              |
|------|------------------------------|
| ESRD | End-Stage Renal Disease      |
| ACR  | Albumin-to-Creatinine Ratio  |
| GBM  | Glomerular Basement Membrane |
| IP3  | inositol 1,4,5-trisphosphate |
| NHE  | Sodium-Hydrogen Exchanger    |
| PAS  | Periodic Acid-Schiff         |
| PKC  | Protein Kinases C            |
| STZ  | Streptozotocin               |
| UPE  | Urinary Protein Excretion    |

|      |                      |
|------|----------------------|
| CrCl | Creatinine Clearance |
| DN   | Diabetic Nephropathy |
| FP   | Foot Processes       |
| SD   | Slit Diaphragm       |
| ZO   | Zonula Occludens     |

## References

1. Fouli, G.E.; Gnudi, L. The Future: Experimental Therapies for Renal Disease in Diabetes. *Nephron* **2018**, 1–5. [[CrossRef](#)] [[PubMed](#)]
2. Koye, D.N.; Magliano, D.J.; Nelson, R.G.; Pavkov, M.E. The Global Epidemiology of Diabetes and Kidney Disease. *Adv. Chronic Kidney Dis.* **2018**, *25*, 121–132. [[CrossRef](#)] [[PubMed](#)]
3. Palsson, R.; Patel, U.D. Cardiovascular complications of diabetic kidney disease. *Adv. Chronic Kidney Dis.* **2014**, *21*, 273–280. [[CrossRef](#)] [[PubMed](#)]
4. Sud, M.; Tangri, N.; Pintilie, M.; Levey, A.S.; Naimark, D. Risk of end-stage renal disease and death after cardiovascular events in chronic kidney disease. *Circulation* **2014**, *130*, 458–465. [[CrossRef](#)] [[PubMed](#)]
5. Yuan, C.M.; Nee, R.; Ceckowski, K.A.; Knight, K.R.; Abbott, K.C. Diabetic nephropathy as the cause of end-stage kidney disease reported on the medical evidence form CMS2728 at a single center. *Clin. Kidney J.* **2017**, *10*, 257–262. [[CrossRef](#)] [[PubMed](#)]
6. Neumiller, J.J.; Alicic, R.Z.; Tuttle, K.R. Therapeutic Considerations for Antihyperglycemic Agents in Diabetic Kidney Disease. *J. Am. Soc. Nephrol.* **2017**, *28*, 2263–2274. [[CrossRef](#)]
7. Gray, S.P.; Jandeleit-Dahm, K. The pathobiology of diabetic vascular complications—cardiovascular and kidney disease. *J. Mol. Med.* **2014**, *92*, 441–452. [[CrossRef](#)]
8. Alicic, R.Z.; Rooney, M.T.; Tuttle, K.R. Diabetic Kidney Disease: Challenges, Progress, and Possibilities. *Clin. J. Am. Soc. Nephrol.* **2017**, *12*, 2032–2045. [[CrossRef](#)] [[PubMed](#)]
9. Grange, C.; Gurrieri, M.; Verta, R.; Fantozzi, R.; Pini, A.; Rosa, A.C. Histamine in the kidneys: What is its role in renal pathophysiology? *Br. J. Pharm.* **2019**. [[CrossRef](#)]
10. Pini, A.; Verta, R.; Grange, C.; Gurrieri, M.; Rosa, A.C. Histamine and diabetic nephropathy: An up-to-date overview. *Clin. Sci. (Lond.)* **2019**, *133*, 41–54. [[CrossRef](#)]
11. Gill, D.S.; Barradas, M.A.; Fonseca, V.A.; Dandona, P. Plasma histamine concentrations are elevated in patients with diabetes mellitus and peripheral vascular disease. *Metabolism* **1989**, *38*, 243–247. [[CrossRef](#)]
12. Alkan, M.; Machavoine, F.; Rignault, R.; Dam, J.; Dy, M.; Thieblemont, N. Histidine Decarboxylase Deficiency Prevents Autoimmune Diabetes in NOD Mice. *J. Diabetes Res.* **2015**, *2015*, 965056. [[CrossRef](#)] [[PubMed](#)]
13. Gill, D.S.; Thompson, C.S.; Dandona, P. Increased histamine in plasma and tissues in diabetic rats. *Diabetes Res.* **1988**, *7*, 31–34. [[PubMed](#)]
14. Gill, D.S.; Thompson, C.S.; Dandona, P. Histamine synthesis and catabolism in various tissues in diabetic rats. *Metabolism* **1990**, *39*, 815–818. [[CrossRef](#)]
15. Pini, A.; Grange, C.; Veglia, E.; Argenziano, M.; Cavalli, R.; Guasti, D.; Calosi, L.; Ghe, C.; Solarino, R.; Thurmond, R.L.; et al. Histamine H4 receptor antagonism prevents the progression of diabetic nephropathy in male DBA2/J mice. *Pharm. Res.* **2018**, *128*, 18–28. [[CrossRef](#)] [[PubMed](#)]
16. Sedor, J.R.; Abboud, H.E. Actions and metabolism of histamine in glomeruli and tubules of the human kidney. *Kidney Int.* **1984**, *26*, 144–152. [[CrossRef](#)]
17. Sedor, J.R.; Abboud, H.E. Histamine modulates contraction and cyclic nucleotides in cultured rat mesangial cells. Differential effects mediated by histamine H1 and H2 receptors. *J. Clin. Investig.* **1985**, *75*, 1679–1689. [[CrossRef](#)]
18. Veglia, E.; Pini, A.; Moggio, A.; Grange, C.; Premoselli, F.; Miglio, G.; Tiligada, K.; Fantozzi, R.; Chazot, P.L.; Rosa, A.C. Histamine type 1-receptor activation by low dose of histamine undermines human glomerular slit diaphragm integrity. *Pharm. Res.* **2016**, *114*, 27–38. [[CrossRef](#)] [[PubMed](#)]
19. Veglia, E.; Grange, C.; Pini, A.; Moggio, A.; Lanzi, C.; Camussi, G.; Chazot, P.L.; Rosa, A.C. Histamine receptor expression in human renal tubules: A comparative pharmacological evaluation. *Inflamm. Res.* **2015**, *64*, 261–270. [[CrossRef](#)]

20. Rosa, A.C.; Grange, C.; Pini, A.; Katebe, M.A.; Benetti, E.; Collino, M.; Miglio, G.; Bani, D.; Camussi, G.; Chazot, P.L.; et al. Overexpression of histamine H(4) receptors in the kidney of diabetic rat. *Inflamm. Res.* **2013**, *62*, 357–365. [[CrossRef](#)] [[PubMed](#)]
21. Pini, A.; Chazot, P.L.; Veglia, E.; Moggio, A.; Rosa, A.C. H3 receptor renal expression in normal and diabetic rats. *Inflamm. Res.* **2015**, *64*, 271–273. [[CrossRef](#)]
22. Gardner, T.W.; Leshner, T.; Khin, S.; Vu, C.; Barber, A.J.; Brennan, W.A., Jr. Histamine reduces ZO-1 tight-junction protein expression in cultured retinal microvascular endothelial cells. *Biochem. J.* **1996**, *320*, 717–721. [[CrossRef](#)] [[PubMed](#)]
23. Ichikawa, I.; Brenner, B.M. Mechanisms of action of histamine and histamine antagonists on the glomerular microcirculation in the rat. *Circ. Res.* **1979**, *45*, 737–745. [[CrossRef](#)]
24. Bolton, W.K.; Spargo, B.A.; Lewis, E.J. Chronic autologous immune complex glomerulopathy: Effect of cyproheptadine. *J. Lab. Clin. Med.* **1974**, *83*, 695–704. [[PubMed](#)]
25. Anbar, H.S.; Shehatou, G.S.; Suddek, G.M.; Gameil, N.M. Comparison of the effects of levocetirizine and losartan on diabetic nephropathy and vascular dysfunction in streptozotocin-induced diabetic rats. *Eur. J. Pharm.* **2016**, *780*, 82–92. [[CrossRef](#)] [[PubMed](#)]
26. Alpers, C.E.; Hudkins, K.L. Mouse models of diabetic nephropathy. *Curr. Opin. Nephrol. Hypertens.* **2011**, *20*, 278–284. [[CrossRef](#)] [[PubMed](#)]
27. Lucero, M.L.; Patterson, A.B. Whole-body tissue distribution of total radioactivity in rats after oral administration of [(1)(4)C]-bilastine. *Drug Chem. Toxicol.* **2012**, *35*, 1–7. [[CrossRef](#)]
28. Wolthers, O.D. Bilastine: A new nonsedating oral H1 antihistamine for treatment of allergic rhinoconjunctivitis and urticaria. *Biomed. Res. Int.* **2013**, *2013*, 626837. [[CrossRef](#)] [[PubMed](#)]
29. Biemesderfer, D.; Pizzonia, J.; Abu-Alfa, A.; Exner, M.; Reilly, R.; Igarashi, P.; Aronson, P.S. NHE3: A Na<sup>+</sup>/H<sup>+</sup> exchanger isoform of renal brush border. *Am. J. Physiol.* **1993**, *265*, F736–F742. [[CrossRef](#)]
30. Banks, R.O.; Inscho, E.W.; Jacobson, E.D. Histamine H1 receptor antagonists inhibit autoregulation of renal blood flow in the dog. *Circ. Res.* **1984**, *54*, 527–535. [[CrossRef](#)]
31. Schulte, K.; Berger, K.; Boor, P.; Jirak, P.; Gelman, I.H.; Arkill, K.P.; Neal, C.R.; Kriz, W.; Floege, J.; Smeets, B.; et al. Origin of parietal podocytes in atubular glomeruli mapped by lineage tracing. *J. Am. Soc. Nephrol.* **2014**, *25*, 129–141. [[CrossRef](#)] [[PubMed](#)]
32. Teng, B.; Duong, M.; Tossidou, I.; Yu, X.; Schiffer, M. Role of protein kinase C in podocytes and development of glomerular damage in diabetic nephropathy. *Front. Endocrinol.* **2014**, *5*, 179. [[CrossRef](#)]
33. Xu, Z.G.; Ryu, D.R.; Yoo, T.H.; Jung, D.S.; Kim, J.J.; Kim, H.J.; Choi, H.Y.; Kim, J.S.; Adler, S.G.; Natarajan, R.; et al. P-Cadherin is decreased in diabetic glomeruli and in glucose-stimulated podocytes in vivo and in vitro studies. *Nephrol. Dial. Transplant.* **2005**, *20*, 524–531. [[CrossRef](#)] [[PubMed](#)]
34. Miethe, S.; Guarino, M.; Alhamdan, F.; Simon, H.U.; Renz, H.; Dufour, J.F.; Potaczek, D.P.; Garn, H. Effects of obesity on asthma: Immunometabolic links. *Pol. Arch. Intern. Med.* **2018**, *128*, 469–477. [[CrossRef](#)] [[PubMed](#)]
35. Klamt, S.; Vogel, M.; Kapellen, T.M.; Hiemisch, A.; Prenzel, F.; Zachariae, S.; Ceglarek, U.; Thiery, J.; Kiess, W. Association between IgE-mediated allergies and diabetes mellitus type 1 in children and adolescents. *Pediatr. Diabetes* **2015**, *16*, 493–503. [[CrossRef](#)] [[PubMed](#)]
36. Potaczek, D.P. Links between allergy and cardiovascular or hemostatic system. *Int. J. Cardiol.* **2014**, *170*, 278–285. [[CrossRef](#)] [[PubMed](#)]
37. Girardi, A.C.; Di Sole, F. Deciphering the mechanisms of the Na<sup>+</sup>/H<sup>+</sup> exchanger-3 regulation in organ dysfunction. *Am. J. Physiol. Cell Physiol.* **2012**, *302*, C1569–C1587. [[CrossRef](#)]
38. Segnani, C.; Ippolito, C.; Antonioli, L.; Pellegrini, C.; Blandizzi, C.; Dolfi, A.; Bernardini, N. Histochemical Detection of Collagen Fibers by Sirius Red/Fast Green Is More Sensitive than van Gieson or Sirius Red Alone in Normal and Inflamed Rat Colon. *Plos ONE* **2015**, *10*, e0144630. [[CrossRef](#)]

